

Hall effect anomaly near T_c and renormalized superconducting fluctuations in $\text{YBa}_2\text{Cu}_3\text{O}_{7-x}$

I. Puica,^{*} W. Lang,[†] and W. Göb

Institut für Materialphysik der Universität Wien, Boltzmannngasse 5, A-1090 Wien, Austria

Roman Sobolewski[‡]

*Department of Electrical and Computer Engineering and Laboratory for Laser Energetics,
University of Rochester, Rochester, New York 14627-0231*

(Dated: February 2, 2008)

Measurements of the Hall effect and the resistivity on precisely-patterned $\text{YBa}_2\text{Cu}_3\text{O}_{7-x}$ thin films in magnetic fields B from 0.5 to 6 T oriented parallel to the sample crystallographic c axis reveal a sign reversal of the Hall coefficient for $B \leq 3$ T. The data are compared to the full, quantitative expressions based on the renormalized fluctuation model for the Hall conductivity. The model offers a satisfactory understanding of the experimental results, for moderate fields and temperatures near the critical region, provided that the inhomogeneity of the critical temperature distribution is also taken into account. We also propose an approach how vortex pinning that strongly affects the magnitude of the Hall coefficient can be incorporated in the model.

I. INTRODUCTION

The influence of superconducting fluctuations on off-diagonal components of the magnetoconductivity tensor (usually denoted as the excess Hall effect) in high-temperature superconductors (HTSC) has received considerable experimental and theoretical attention over the past few years.^{1,2,3,4,5,6,7,8} Though a general consensus seems to be achieved now regarding the existence and the temperature dependence of the excess Hall effect, theoretical predictions of its sign are still controversial. Experimentally, the Hall resistivity shows a peculiar temperature dependence. Specifically, as the temperature is decreased through the fluctuation region, the Hall resistivity decreases and changes its sign relatively to the normal state one, exhibits a negative minimum and eventually reaches zero at low temperatures. This simple sign change was detected in many different HTSC^{6,8,9,10,11} and even in conventional superconductors.^{7,12,13} Furthermore, a double sign reversal, that is a subsequent return of the Hall resistivity to the positive value before vanishing, has been observed in highly anisotropic HTSC, such as $\text{Bi}_2\text{Sr}_2\text{CaCu}_2\text{O}_x$ crystals¹⁴ and films,¹⁵ $\text{Tl}_2\text{Ba}_2\text{CaCu}_2\text{O}_x$ films,¹⁶ or $\text{HgBa}_2\text{CaCu}_2\text{O}_6$ films.¹⁷ Recently, the existence of the second sign change was also reported in $\text{YBa}_2\text{Cu}_3\text{O}_{7-x}$ films, either at high current densities¹⁸ or in the strong pinning limit at low magnetic fields.¹⁹ Finally, even a triple sign reversal was reported in $\text{HgBa}_2\text{CaCu}_2\text{O}_6$ films with columnar defects induced by high-density ion irradiation.²⁰

Several theoretical approaches have attempted to explain the complex features of the Hall resistivity temperature dependence, but no consensus has been achieved. The Hall anomaly might originate from the pinning force,¹ non-uniform carrier density in the vortex core,^{21,22} or can be calculated in the time-dependent Ginzburg-Landau (TDGL) model.^{23,24} Most recent theories claim to predict the double or triple sign reversal, based ei-

ther on entirely intrinsic mechanism of vortex motion and electronic spectrum,²⁵ or on hydrodynamic interaction between vortices and the superconducting and normal state fluids.²⁶ Some theories invoke superconducting fluctuations alone to account for the Hall effect sign reversal^{27,28}, while others present a more extended picture based on the same foundations of TDGL using both the hydrodynamics and the vortex charging effect, arising from the difference in electron density between the core and the far outside region of the vortex.^{21,22,29} Thus, the Hall effect in the mixed state of HTSC reflects a complex interplay between electronic properties of quasiparticles, thermodynamic fluctuations, hydrodynamic effects of vortices, and pinning.

From a considerable part of the published theoretical work, it appears that at least the first sign reversal, which occurs near the critical region, where vortex pinning is negligible and the superconducting order parameter fluctuations play an important role, should be ascribed to a microscopic origin of superconductivity.^{4,13,30,31} From the viewpoint of the TDGL formalism,^{24,27,28} to which any theory of vortex dynamics must reduce near the critical temperature T_c ,^{25,32} the Hall anomaly is a consequence of the difference in sign between the normal (quasiparticle) part and the superconducting fluctuation (or vortex flow) part of the total Hall conductivity. These two components have opposite signs, if the energy derivative of the density of states averaged over the Fermi surface is positive when the carriers are holes in the normal state.³³ Thus, the sign reversal can be intrinsic and depends on the details of the structure of the normal-state electronic spectrum. Such notion is further supported by the fact that in several HTSC, the sign reversal disappears when the material is strongly overdoped and the band structure approaches that of a conventional metal.³⁴

The possibility of the Hall angle sign change in the critical region was first discussed by Fukuyama, Ebisawa and Tsuzuki (FET),³⁵ who pointed out that the origin of

a non-vanishing Hall current due to fluctuating Cooper pairs could come from a hole-particle asymmetry, which reveals a complex relaxation time in the TDGL theory. In this early work, it was implicitly assumed that the fluctuations did not interact; that is, only Gaussian fluctuation were considered. Accordingly, the fluctuation parts of the conductivity tensor elements were predicted to diverge at T_c in the presence of magnetic field. However, this predicted divergence has not been observed. A great improvement was obtained when the interaction between fluctuations was taken into account by incorporating the quartic term $|\psi|^4$ from the Ginzburg-Landau (GL) expression of the free energy. Such a treatment was performed by Ullah and Dorsey²⁷ (UD) in the frame of a simple Hartree approach of the TDGL theory. More recently, Nishio and Ebisawa²⁸ (NE) extended the FET calculations of the weak (Gaussian) fluctuation contribution of the Hall conductivity to the strong (non-Gaussian) fluctuation regime, based on more sophisticated renormalization theory by Ikeda, Ohmi and Tsuneto (IOT).³⁶ The renormalized, non-Gaussian fluctuation regime connects therefore the weak (Gaussian) fluctuation regime in the paraconducting region above $T_{c2}(H)$ to the vortex liquid (flux-flow) regime below the mean-field transition, interpolating smoothly without the T_c divergence predicted by the Gaussian theory.

In this paper, we present simultaneous measurements of the resistivity and Hall resistivity, of epitaxial $\text{YBa}_2\text{Cu}_3\text{O}_{7-x}$ (YBCO) films in a wide range of applied magnetic fields (from 0.5 to 6 T), and give a quantitative account for our Hall-effect experimental data by using the aforementioned renormalized fluctuation model of NE.²⁸ It is worth mentioning that for $B < 0.5$ T, we have earlier found an occurrence of the second sign reversal¹⁹ in similar YBCO thin films in B fields oriented parallel to the crystallographic c axis and to the twin boundaries. This second sign change turned out to be strongly vortex-pinning dependent, since it vanished at high transport current densities, or with the B field tilted off the twin boundaries by a small angle (5°). For moderate magnetic fields instead, as those investigated in the present paper, and for temperatures near the critical region, where the first sign change occurs, the pinning contribution to the Hall conductivity is almost negligible.¹⁹ The TDGL approach is therefore considered to be appropriate, although quantitatively less accurate towards lower temperatures and fields, where pinning becomes more effective.

There have been so far several reported verifications of merely scaling relationships connecting fluctuation conductivities, temperature, and magnetic field, emerging from the TDGL model. Liu *et al.*⁵ found good experimental evidence for the validity of the scaling laws depending on temperature and B field given by the Hartree renormalization procedure in the lowest Landau level.²⁷ This approach was applied to the Aslamazov-Larkin (AL) term of the fluctuation longitudinal and Hall conductivities,³⁷ for B fields ranging between 2 and

9 T, and identified the cause of the Hall conductivity sign change as lying in the fluctuation regime. Ginsberg and Manson³⁸ and Neiman *et al.*,³⁹ also found a satisfactory fit for their data by using the $1/B$ proportionality of the fluctuation Hall conductivity, predicted by the same Hartree renormalization fluctuation model²⁷ in the lowest Landau level approximation (valid in the high field limit). We have, however, no knowledge of any direct comparison between experimentally observed Hall anomaly in HTSC and the full quantitative application of the TDGL theory in the renormalized fluctuation regime, where the first sign reversal occurs. And this is the main purpose of this work. In Sec. II, the most important results of the IOT³⁶ and NE²⁸ renormalized fluctuation theories for the longitudinal and Hall conductivities are reviewed, and modifications for including samples with nonuniform T_c 's are proposed. Section III briefly presents our sample preparation and measurement techniques, while Sec. IV shows our experimental results and directly compares them to the theoretical model. Finally, in Sec. V, we summarize our results and list the main conclusions emerging from our analysis.

II. THEORETICAL BACKGROUND

Based on the IOT renormalization theory, NE extended FET calculations of the weak fluctuation contribution of Hall conductivity and derived an expression of the excess Hall conductivity $\Delta\sigma_{xy}$ due to the non-Gaussian superconducting fluctuations corresponding to the AL process in a layered superconductor:

$$\Delta\sigma_{xy} = \beta \frac{e^2 h^3}{\hbar \xi_c} \frac{k_B T}{\varepsilon_F} \sum_{n=0}^{\infty} \frac{(n+1)}{(\varepsilon_{n+1} - \varepsilon_n)^2} \times [1 + d^2(\varepsilon_n + \varepsilon_{n+1})] \left(\frac{f_n^2 f_{n+1}^2}{f_n + f_{n+1}} - \frac{1}{2} f_{n+\frac{1}{2}}^3 \right), \quad (1)$$

with: $f_n = [\varepsilon_n (1 + d^2 \varepsilon_n)]^{-1/2}$; $\varepsilon_n = \varepsilon_0 + 2nh$, ($n \geq 1$); $\varepsilon_0 = \varepsilon + h$; $\varepsilon = (T - T_c)/T_c$; $h = 2\pi \xi_{ab}^2 B/\Phi_0$; $d = s/2\xi_c$; $\beta = -4\varepsilon_F N'/\pi g N^2$. Here N is the density of states at the Fermi surface ε_F , N' is the energy derivative of N , g (> 0) the BCS coupling constant, ξ_{ab} and ξ_c are the coherence lengths extrapolated at $T = 0$ in ab and c directions, respectively, s is the distance between superconductor layers in the Lawrence-Doniach⁴⁰ model, T_c is the critical temperature in the absence of the magnetic field, and B the magnetic field applied perpendicularly to the ab plane. The renormalization procedure, described in detail by IOT, consists in using the renormalized expression $\tilde{\varepsilon}_n$ instead of ε_n for each Landau level n ,

$$\begin{aligned} \tilde{\varepsilon}_n &= \varepsilon_n + \frac{g_3 d}{\sqrt{\beta_0^2 - 1}} + \frac{\sqrt{\beta_0^2 - 1}}{8\beta_0 d^2 (n+1)!} \\ &\times \left\{ \left(\ln \frac{\gamma_+}{\alpha_+} \right)^{n+1} + \frac{\alpha - \beta_0}{\sqrt{\beta_0^2 - 1}} \right. \\ &\times \left. \left[\ln \left(\frac{\beta_0 \gamma + \sqrt{(\beta_0^2 - 1)(\gamma^2 - 1)} - 1}{\beta_0 \alpha + \sqrt{(\beta_0^2 - 1)(\alpha^2 - 1)} - 1} \right) \right]^{n+1} \right\} \end{aligned} \quad (2)$$

where: $g_3 = 8\pi^2 \mu_0 \kappa^2 k_B T_c \xi_{ab}^4 B / \xi_c \Phi_0^3$; $\beta_0 = 1 + 2d^2 \tilde{\varepsilon}_0$; $\alpha = 2\beta_0^2 - 1$; $\gamma = \alpha + 8g_3 \beta_0 d^3 (\beta_0^2 - 1)^{-1/2}$; $\alpha_+ = \alpha + \sqrt{\alpha^2 - 1}$; $\gamma_+ = \gamma + \sqrt{\gamma^2 - 1}$, and κ being the GL parameter of the superconductor. The second term on the right hand side of Eq. (2) is the Hartree term and always dominates the third one.

The pre-factor in Eq. (1) can be modified in a form more convenient for experimental data fits. Taking into account the coherence length expression valid in the dirty limit:⁴¹ $\xi_{ab} = (\pi \hbar v_F l / 24 k_B T_c)^{1/2}$ (where v_F is the Fermi velocity, τ the scattering time and $l = v_F \tau$ is the mean free path) together with the normal-state Hall conductivity expression in the classical picture:³⁵ $\sigma_{xy}^n = \sigma_{xx}^n e B \tau / m_e$, one can obtain the following form for $\Delta \sigma_{xy}$ when $T \approx T_c$:

$$\begin{aligned} \Delta \sigma_{xy} &= \beta \frac{\pi e^2}{24 \hbar \xi_c} \cdot \frac{\sigma_{xy}^n}{\sigma_{xx}^n} \cdot \sum_{n=0}^{\infty} \frac{4h^2 (n+1)}{(\tilde{\varepsilon}_{n+1} - \tilde{\varepsilon}_n)^2} \\ &\times [1 + d^2 (\tilde{\varepsilon}_n + \tilde{\varepsilon}_{n+1})] \left(\frac{\tilde{f}_n^2 \tilde{f}_{n+1}^2}{\tilde{f}_n + \tilde{f}_{n+1}} - \frac{1}{2} \tilde{f}_{n+\frac{1}{2}}^3 \right) \end{aligned} \quad (3)$$

with $\tilde{f}_n = [\tilde{\varepsilon}_n (1 + d^2 \tilde{\varepsilon}_n)]^{-1/2}$ and $\tilde{\varepsilon}_n$ given by Eq. (2). Expression (3) concerns, as stated, a layered superconductor, and only the pre-factor was computed assuming a three-dimensional (3D) isotropic Fermi surface, as in the BCS theory, justified by the moderate YBCO anisotropy. Considering instead a cylindrical Fermi surface, corresponding to the two-dimensional (2D) case, would change the ξ_{ab} expression by a factor of $\sqrt{3/2}$,⁴¹ and consequently the β value by a factor of 2/3. Since the correct band structure for YBCO is expected to be in between these two limit cases, our estimation for β will be only slightly affected. Noticing that $\tilde{\varepsilon}_{n+1} - \tilde{\varepsilon}_n \approx 2h$, one can verify that the above formula gives in the low-field limit ($h \ll \varepsilon$) in the paraconducting region (above T_c), an expression that formally matches the 2D and 3D results of the FET theory for the AL fluctuation term. The 2D limit corresponds to $\varepsilon d^2 \gg 1$, while the 3D limit is valid when $\varepsilon d^2 \ll 1$. The essential difference remains, however, the presence in Eq. (3) of the ε_n -renormalization, according to the IOT theory of non-Gaussian superconducting fluctuations.

The IOT theory also gives the fluctuation contribution to the longitudinal conductivity in the renormalized

regime:

$$\Delta \sigma_{xx} = \frac{e^2 h^2}{2 \hbar \xi_c} \sum_{n=0}^{\infty} \frac{n+1}{(\tilde{\varepsilon}_{n+1} - \tilde{\varepsilon}_n)^2} (\tilde{f}_n + \tilde{f}_{n+1} - 2\tilde{f}_{n+\frac{1}{2}}) \quad (4)$$

which, as derived from the GL functional, corresponds to the AL process. It is worth mentioning that the sums over Landau levels in Eqs. (1) and (4) given by the IOT - NE theory correspond formally to those found in the results of UD²⁷ in the frame of a simple Hartree approach for incorporating the $|\psi|^4$ term in the TDGL theory, with the specification that the UD renormalization procedure retains only the Hartree contribution.

In previous papers,^{42,43} it was reported that even minor inhomogeneities of T_c within the sample may have a measurable, quantitative effect to the paraconductivity, fluctuation magnetoconductivity, and excess Hall conductivity. Thus, we are going to take this effect into account in our derivations. Retaining only the first order expansion term of the effective medium approximation, the inhomogeneity correction writes simply as an average of fluctuation conductivities over the T_c distribution. For simplicity, we assume in our analysis a Gaussian distribution of T_c 's with a mean value T_{c0} and a standard deviation $\delta T_c \ll T_{c0}$, so that the mean fluctuation conductivities will write as:

$$\langle \Delta \sigma \rangle = \int \frac{1}{\delta T_c \sqrt{2\pi}} \exp \left[-\frac{(T_c - T_{c0})^2}{2(\delta T_c)^2} \right] \cdot \Delta \sigma(T_c) dT_c, \quad (5)$$

where $\Delta \sigma$ stands for both $\Delta \sigma_{xy}$ and $\Delta \sigma_{xx}$.

The averaged fluctuation conductivities $\langle \Delta \sigma_{xy} \rangle$ and $\langle \Delta \sigma_{xx} \rangle$ derived from Eqs. (3), (4) and (5) have to be added to the normal state components, σ_{xy}^n and σ_{xx}^n , respectively. No general consensus exists about the functional form of σ_{xx}^n for HTSC, but the linear temperature dependence of resistivity over a broad temperature range is generally accepted. It has also been shown⁴⁴ that many Hall effect measurements in various HTSC materials can be explained using the Anderson's formula:⁴⁵ $\cot \theta_H^n = \sigma_{xx}^n / \sigma_{xy}^n = C_1 T^2 + C_0$. We shall therefore use for the normal-state part of the conductivity tensor the simple expressions:

$$\sigma_{xx}^n = \frac{1}{p_0 + p_1 T} \quad \text{and} \quad \sigma_{xy}^n = \frac{1}{p_0 + p_1 T} \cdot \frac{1}{C_1 T^2 + C_0}, \quad (6)$$

where p_0 , p_1 , C_1 and C_0 are fitting parameters to be determined from the experiment. Thus, the full conductivities will be consequently:

$$\sigma_{xx} = \sigma_{xx}^n + \langle \Delta \sigma_{xx} \rangle \quad \text{and} \quad \sigma_{xy} = \sigma_{xy}^n + \langle \Delta \sigma_{xy} \rangle, \quad (7)$$

where $\langle \Delta \sigma_{xy} \rangle$ is given by Eqs. (3) and (5), $\langle \Delta \sigma_{xx} \rangle$ by Eqs. (4) and (5), and σ_{xy}^n and σ_{xx}^n by Eq. (6).

In the above considerations, we only included the AL process as contribution to the fluctuation Hall and longitudinal conductivities. In order not to overcomplicate

the model by introducing non-essential parameters, we neglect the Maki-Thompson⁴⁶ and the density-of-states terms,⁴⁷ which contribute as corrections to the excess conductivities only when $B \ll 1$ T, and only in the above- T_c region. They give therefore a negligible contribution to the sign change features of the Hall resistivity, and, moreover, their influence can hardly be quantitatively discerned from a small correction of the normal-state fit.

III. EXPERIMENTAL TECHNIQUES

Our epitaxial YBCO thin films were deposited by single-target rf sputtering on LaAlO_3 substrates and patterned to precisely aligned test structures using a laser inhibition technique on a computer-controlled xy-stage.⁴⁸ Electrical contacts were established with gold wires, attached by silver paste to evaporated silver pads. The onset of the superconducting transition in zero field was at 90 K and the critical current density of our films exceeded 3 MA/cm² at 77 K.

The experiments were performed with 17-Hz ac currents at $j = 250$ A/cm² together with lock-in detection. The measurements from 1 to 6 T were made in a commercial superconducting solenoid, while low-field measurements at 0.5 and 1 T were performed in a closed-cycle cryocooler and with an electromagnet. Results obtained from these two different set-ups were identical at $B = 1$ T. More detailed description of our experimental systems can be found in Refs. 19 and 48.

IV. RESULTS AND DISCUSSIONS

The experimental Hall resistivity normalized to the field for a YBCO thin film, measured in various magnetic fields is shown in Fig. 1 (symbols), while in the inset in Fig. 1 the longitudinal resistivity is presented (symbols). The superconducting transition in Fig. 1 inset is typical for a thin-film sample with a vortex-glass behavior at low temperatures, while the shape of the upper part of the transition is common to both thin films and single crystals.⁴⁹ Figure 1 shows that the Hall resistivity is always positive (hole-like) for $B > 3$ T and exhibits the sign change at lower fields, in accordance with previous investigations performed in the similar magnetic field range. One can also notice that the Hall resistivity minimum occurs in the vortex-liquid regime, and that the Hall anomaly increases significantly when the field is reduced below 2 T.

Our first attempt to fit the experimental data by using theoretical dependencies of the renormalized fluctuation model^{27,28} is also shown in Fig. 1 (dotted lines) and results in curves similar to those presented in the IOT and NE theoretical papers. The effect of the sample inhomogeneity was in this approach neglected. Eq. (4), given by the IOT model, was used for the fluctuation longitudinal conductivity, while Eq. (3), based on the NE model, pro-

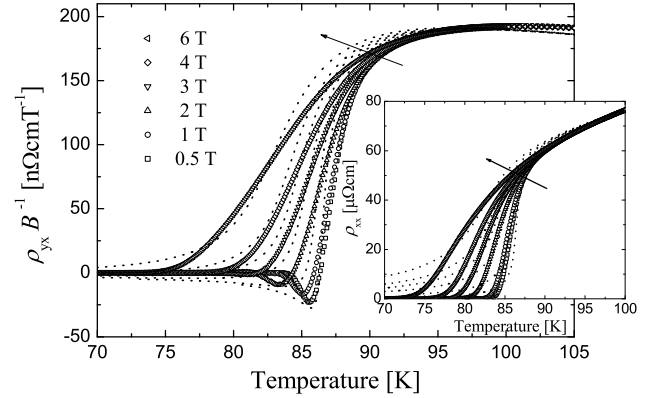


FIG. 1: Comparison between the experiment (symbols) and the NE renormalized fluctuation model (dotted lines) for the YBCO normalized Hall resistivity ρ_{yx}/B as a function of temperature for different values of the magnetic field. The inset shows the comparison between the experiment (symbols) and the IOT renormalized fluctuation model (dotted lines) for the YBCO longitudinal resistivity ρ_{xx} . The arrows indicate the increasing field direction. The fit parameters are given in the text.

vided the fluctuation Hall conductivity. Both models rely on the same set of adjustable parameters. The normal state contributions, obtained by fitting the experimental data for temperatures greater than 100 K with the expressions given in Eq. (6), were, subsequently, added to the fluctuation contributions. Finally, the inverted conductivity tensor gave the longitudinal and Hall conductivity shown in Fig. 1. The model parameters that allowed to find the best fitting theoretical curves, were: $T_c = 87$ K, $\kappa = 70$, $s = 1.17$ nm equal to the c -axis lattice parameter (this implies that the two copper-oxide planes in the unit cell are tightly coupled, acting as one superconducting layer), $\xi_{ab} = 1.2$ nm and $\xi_c = 0.14$ nm at $T = 0$, and $\beta = -0.007$. Comparison between the experiment and the model in Fig. 1 shows that the renormalized fluctuation approach is adequate, at least from a qualitative point of view. All features of the Hall resistivity dependence on temperature, namely the steep decrease in the fluctuation region below 90 K, the sign change, the negative minimum and subsequently the vanishing trend at low temperatures are clearly reproduced by the model.

We note that the fitting parameters listed above, like the coherence lengths and the Ginzburg-Landau parameter assume the values very typical for YBCO. Essential for this approach is, however, the negative value of the hole-particle asymmetry parameter β (this means a negative $\Delta\sigma_{xy}$) that implies a positive energy derivative of the density of states at ε_F when the carriers are holes in the normal state. As suggested by Kopnin and Vinokur,⁵⁰ one possibility to explain this behaviour is that the Fermi surface of a metal in the normal state has both hole-like

and electronic pockets. The Hall anomaly may thus depend on the doping level, as it was reported by Nagaoka *et al.*³⁴ Very recently, Angilella *et al.*⁵¹ have found that, close to an electronic topological transition of the Fermi surface, in the hole-like doping range, the fluctuation Hall conductivity has indeed an opposite sign with respect to the normal state one, giving additional strong support that the Hall resistivity sign reversal is intrinsic and depends on the details of the structure of the electronic spectrum.

We shall further discuss the reasons for quantitative discrepancies between experimental curves and the model predictions in Fig. 1, and provide some modalities to improve them. A first point is that the IOT model for the longitudinal resistivity fails to reproduce correctly the low temperature part of the transition, giving too long tail of the resistivity decrease. Two reasons are responsible for this behavior. One of them lies in the renormalization procedure in the IOT model, which roughly corresponds to a Hartree approximation. As remarked by Ullah and Dorsey,²⁷ an important consequence of the Hartree approximation is that the calculated properties in the flux-flow limit differ from the mean-field predictions by a numerical factor of $2/\beta_A$, where β_A is the Abrikosov parameter $\beta_A = \langle |\psi|^4 \rangle / \langle |\psi|^2 \rangle^2 = 1.16$ for a triangular vortex lattice. Thus, the Hartree prediction for the conductivity is $2/\beta_A$ times smaller than the mean field result, which consequently leads to a higher resistivity predicted by the fluctuation model in the low-temperature range of the transition, as it can be seen in the inset in Fig. 1. Another reason, maybe more important quantitatively, is the presence of flux pinning, which is neglected in the fluctuation model, but which drastically steeps the resistivity descent in the lower part of the transition. This quantitative inadequacy of the fluctuation model for the ρ_{xx} in the low temperature region manifests itself implicitly in the corresponding features of the ρ_{yx} theoretical curve, namely in the long, nonvanishing tail at low temperatures. For this reason, we decided to further test the general validity of the renormalized fluctuation model over the entire temperature range only for the Hall conductivity $\sigma_{xy} = \rho_{yx} / (\rho_{xx}^2 + \rho_{yx}^2)$ that is believed to be almost independent of pinning.²

Following the above conclusion, Fig. 2 (symbols) presents the experimental Hall conductivity σ_{xy} normalized to B . It is instructive to visualize the Hall effect using this plot, since σ_{xy}/B is independent of B in the normal state above 90 K. The observed behavior suggests the presence of at least two contributions to the Hall conductivity. One has the same sign as the normal-state effect and rapidly increases below $T_c(B)$, becoming predominant for $B > 4$ T, and indicating a reduced carrier scattering in the superconducting state. The other contribution exhibits an opposite sign and gains importance with smaller B 's. Thus, for fields smaller than 3 T, the negative part dominates and σ_{xy} changes its sign. It can be also noticed in Fig. 2 that with decreasing B , the

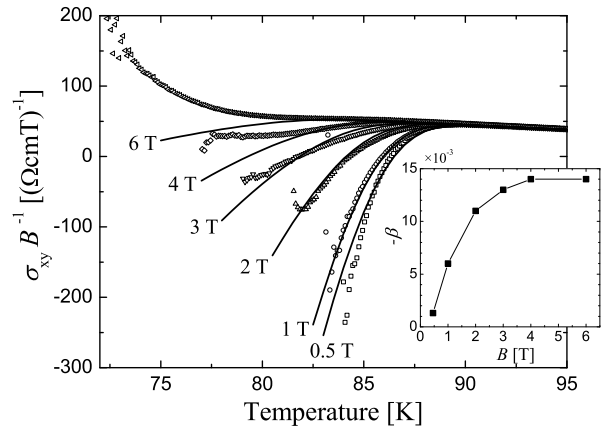


FIG. 2: Comparison between the experiment (symbols) and the renormalized fluctuation model (solid lines) for the YBCO normalized Hall conductivity σ_{xy}/B as a function of temperature for different values of the magnetic field. The NE model was used here with the relaxed β parameter, in order to obtain the best fit. An average of the Hall conductivities over a Gaussian distribution of T_c 's within the sample was also included. The inset shows the β dependence on the magnetic field, extracted from fitting. The line is to guide the eye.

negative contribution shifts to higher temperatures and exists in a narrower temperature range.

In small B fields, the Hall anomaly is a very sharp feature in the experimental data. A possible inhomogeneity of the material will influence the low-field results, but remain insignificant at higher fields. In order to improve the quantitative agreement with the experiment, we have included in our model a distribution of T_c 's over the sample [see Eq. (5)], and Eq. (7) was used for the Hall conductivity. The main effects of this correction are a less steep decrease of the Hall resistivity in the first part of the transition (immediately below 90 K) and a relative reduction in absolute value of the negative minimum. Figure 2 presents the results of such a model (solid lines), where a Gaussian distribution of T_c 's was used with a relative variance $\delta T_c/T_{c0} = 0.02$. All the other parameters except β , namely ξ_{ab} , ξ_c , s and κ remained the same, as used in the fits shown in Fig. 1. We found that the best fits were obtained with a relaxed β parameter, and inferred empirically an apparent field dependence of this parameter, shown in the inset in Fig. 2. We think, however that the decrease of the β absolute value with decreasing B could be simply the dissimulated effect of the increasing role of vortex pinning at lower field values. Indeed, in our recent paper,¹⁹ a second sign reversal was clearly identified for fields under 0.5 T and this effect became more important with the decreasing field. The second sign change disappeared in high current densities or under slightly tilted field direction, revealing its vortex pinning origin. The positive pinning contribution to the Hall conductivity, which gains importance at low fields could

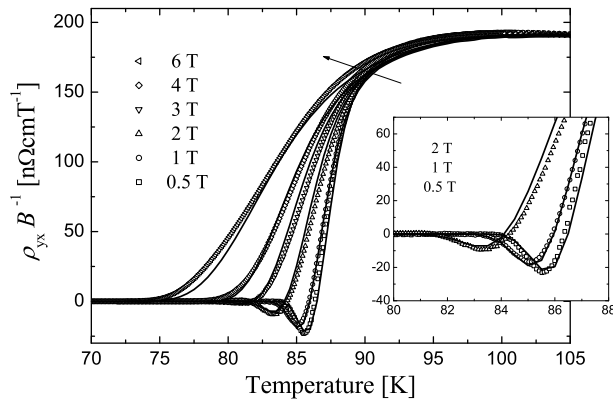


FIG. 3: Comparison between the experiment (symbols) and the renormalized fluctuation model (solid lines) for the YBCO normalized Hall resistivity ρ_{yx}/B as a function of temperature for different values of the magnetic field (the arrow indicates the increasing B direction). The experimental longitudinal conductivity was used for the calculation of ρ_{yx} . The inset shows the transition temperature region in detail. For further details see the text.

be therefore reflected in the apparent field-dependence of the absolute value of β . In a recent theoretical work, Kopnin and Vinokur⁵⁰ also signalized, based on a simple model of pinning potential, that an increasing pinning strength not only affected the longitudinal flux-flow resistivity, but also decreased the magnitude of the vortex contribution to the Hall voltage (fluctuation term in the TDGL approach). Strong enough pinning can even result in a second sign reversal of the Hall resistivity, if the negative vortex (fluctuation) contribution is reduced in absolute value to magnitudes that are insufficient to counteract the positive contribution of the normal state conduction.^{32,50}

The best illustration of our modelling approach is presented in Fig. 3 where we show the normalized Hall resistivity ρ_{yx}/B computed by using the *theoretical* Hall conductivity $\sigma_{xy} = \sigma_{xy}^n + \langle \Delta \sigma_{xy} \rangle$ and the *experimental* longitudinal conductivity $\sigma_{xx}^{\text{exp}} \cong 1/\rho_{xx}^{\text{exp}}$, with the T_c -distribution correction included. The idea behind this procedure is that the effect of pinning manifests itself primarily in σ_{xx} , whereas σ_{xy} is almost independent of pinning for magnetic fields ≥ 1 T, as it was shown in a number of different experiments using artificially introduced defects^{4,31} or variation of current density.³⁰ We note an extremely good agreement between the experimental and theoretical curves of the Hall resistivity in the entire temperature and magnetic field ranges. For fields above 3 T, for which the transition width enlarges towards lower temperatures (below 80 K), an additional positive contribution to the Hall conductivity (see Fig. 2), other than the extrapolation of the normal state one, turns out to play a prevalent role. This effect is now not evidenced in the Hall resistivity picture (Fig. 3), due to

the vanishing Hall resistivity in this temperature region. A possible interpretation for this supplementary positive term to the Hall conductivity is the modification of the normal-state conduction itself, namely, a reduced carrier scattering of quasiparticles in the superconducting state. Figure 3 also proves that the much slower asymptotic trend of the theoretical Hall resistivity towards zero observed in Fig. 1, was indeed caused by the non-adequacy of the fluctuation model to the low-temperature part of the longitudinal resistivity dependence. An improvement of the model should therefore take into account also flux pinning, since it affects the longitudinal conductivity in the lower part of the transition. It can also be seen comparing Figs. 2 and 3 that including the T_c distribution results in smoothing of the curves and leads to a gentler slope of the Hall resistivity in its initial positive part. Still non-elucidated remains the true value of the β parameter, since the values returned by the fitting procedure are most likely altered by the pinning effect on the Hall conduction and appear to be rather sensitive to sample T_c inhomogeneities. The hole-particle parameter was also deduced from an independent analysis of the excess Hall effect caused by Gaussian superconducting fluctuations above the mean-field critical temperature.³ Although the negative sign was found as well, the magnitude of β differed significantly, likely due to the different limits in the models on which the analysis was based. The negative sign of β , connected with a positive derivative of the density of states at the Fermi level is, however, essential in order to explain the sign change, from positive (hole-like) to negative (electron-like) in the Hall resistivity.

V. CONCLUSIONS

We presented results of simultaneous measurements of the resistivity and Hall resistivity for epitaxial $\text{YBa}_2\text{Cu}_3\text{O}_{7-x}$ films in a wide range of the magnetic field, and explained our Hall-effect experimental data by comparing them to the full quantitative expressions given by the renormalized fluctuation model for the excess Hall conductivity in HTSC materials. We found that this model offers an adequate quantitative understanding of the experimental dependencies for moderate fields and temperatures near the critical region, provided that the inhomogeneity of the T_c distribution is also taken into account. The essential factor that explains the Hall anomaly is the negative fluctuation term in the Hall conductivity, due in turn to the negative hole-particle asymmetry parameter. In this framework, the Hall resistivity sign change and the presence of the negative minimum for magnetic fields lower than 3 T is easily accounted for. We have also found that for high fields ($B \geq 4$ T), in the lowest temperature range of the transition, the positive contribution to the Hall conductivity becomes again prevalent, being greater than the extrapolation of the normal state expression, and giving the evidence for a reduced carrier scattering in the superconducting state.

The conclusion of our analysis is that the Hall anomaly in YBCO thin films is the result of a delicate interplay of three contributions to the Hall conductivity: (i) positive quasiparticle vortex-core contribution, associated with normal-state excitations, which dominates at high fields ($B > 3$ T) and increases above the extrapolation from the normal state below T_c , indicating reduced quasiparticle scattering in superconductor state; (ii) superconducting contribution (excess Hall effect), resulting from the vortex flux-flow and superconducting fluctuations, which, by its negative sign, is connected to the details of the Fermi surface, and is essential to the sign change occurrence in fields below 3 T; and (iii) pinning contribution, which does not contribute significantly to the Hall conductivity in the investigated range of magnetic fields and temperatures, but results in an apparent decrease of the hole-particle asymmetry at low fields. The pinning contribution eventually leads to the second sign reversal of the

Hall effect in YBCO in very low fields ($B < 0.5$ T). Finally, we have found that using the experimental values of σ_{xx} in the calculation of the Hall resistivity removes the apparent quantitative discrepancy between the NE model and the experimental data.

Acknowledgments

This work was supported by the Austrian Fonds zur Förderung der wissenschaftlichen Forschung (Vienna) and by the NSF Grant No. DMR-0073366 (Rochester). Stimulating correspondence and discussions with R. Ikeda, A.A. Varlamov, Y. Matsuda and J. Kolacek, are gratefully acknowledged. We would also like to thank H. Ebisawa for sending their manuscript prior to publication.

-
- * Also at the Department of Physics, Polytechnic University of Bucharest, Spl. Independentei 313, RO-77206 Bucharest 6, Romania
- † Electronic address: wolfgang.lang@univie.ac.at
- ‡ Also at the Institute of Physics, Polish Academy of Sciences, PL-02668 Warszawa, Poland
- ¹ Z. D. Wang, J. M. Dong, and C. S. Ting, Phys. Rev. Lett. **72**, 3875 (1994).
 - ² V. M. Vinokur, V. B. Geshkenbein, M. V. Feigelman, and G. Blatter, Phys. Rev. Lett. **71**, 1242 (1993).
 - ³ W. Lang, G. Heine, P. Schwab, X. Z. Wang, and D. Bäuerle, Phys. Rev. B **49**, 4209 (1994).
 - ⁴ A. V. Samoilov, A. Legris, F. Rullier-Albenque, P. Lejay, S. Bouffard, Z. G. Ivanov, and L.-G. Johansson, Phys. Rev. Lett. **74**, 2351 (1995).
 - ⁵ W. Liu, T. W. Clinton, A. W. Smith, and C. J. Lobb, Phys. Rev. B **55**, 11802 (1997).
 - ⁶ J. Roa-Rojas, P. Prieto, and P. Pureur, Mod. Phys. Lett. **15**, 1117 (2001).
 - ⁷ N. Kokubo, J. Aarts, and P. H. Kes, Phys. Rev. B **64**, 014507 (2001).
 - ⁸ W. N. Kang, D. H. Kim, S. Y. Shim, J. H. Park, T. S. Hahn, S. S. Choi, W. C. Lee, J. D. Hettinger, K. E. Gray, and B. Glagola, Phys. Rev. Lett. **76**, 2993 (1996).
 - ⁹ J. P. Rice, N. Rigakis, D. M. Ginsberg, and J. M. Mochel, Phys. Rev. B **46**, 11050 (1992).
 - ¹⁰ T. W. Clinton, A. W. Smith, Q. Li, J. L. Peng, R. L. Greene, C. J. Lobb, M. Eddy, and C. C. Tsuei, Phys. Rev. B **52**, R7046 (1995).
 - ¹¹ Y. Matsuda, T. Nagaoka, G. Suzuki, K. Kimagai, M. Suzuki, M. Machida, M. Sera, M. Hiroi, and N. Kobayashi, Phys. Rev. B **52**, R15749 (1995).
 - ¹² S. J. Hagen, C. J. Lobb, R. L. Greene, M. G. Forrester, and J. H. Kang, Phys. Rev. B **41**, 11630 (1990).
 - ¹³ J. M. Graybeal, J. Luo, and W. R. White, Phys. Rev. B **49**, 12923 (1994).
 - ¹⁴ A. V. Samoilov, Phys. Rev. Lett. **71**, 617 (1993).
 - ¹⁵ N. V. Zavaritsky, A. V. Samoilov, and A. A. Yurgens, Physica C **180**, 417 (1991).
 - ¹⁶ S. J. Hagen, C. J. Lobb, and R. L. Greene, Phys. Rev. B **43**, 6246 (1991).
 - ¹⁷ W. N. Kang, S. H. Yun, J. Z. Wu, and D. H. Kim, Phys. Rev. B **55**, 621 (1997).
 - ¹⁸ K. Nakao, K. Hayashi, T. Utagawa, Y. Enomoto, and N. Koshi-zuka, Phys. Rev. B **57**, 8662 (1998).
 - ¹⁹ W. Göb, W. Liebich, W. Lang, I. Puica, R. Sobolewski, R. Rössler, J. D. Pedarning, and D. Bäuerle, Phys. Rev. B **62**, 9780 (2000).
 - ²⁰ W. N. Kang, B. W. Kang, Q. Y. Chen, J. Z. Wu, Y. Bai, W. K. Chu, and S.-I. Lee, Phys. Rev. B **61**, 722 (2000).
 - ²¹ A. van Otterlo, M. V. Feigelman, V. B. Geshkenbein, and G. Blatter, Phys. Rev. Lett. **75**, 3736 (1995).
 - ²² Y. Kato, J. Phys. Soc. Japan **68**, 3798 (1999).
 - ²³ R. J. Troy and A. T. Dorsey, Phys. Rev. B **47**, 2715 (1993).
 - ²⁴ N. B. Kopnin, B. I. Ivlev, and V. A. Kalatski, J. Low Temp. Phys. **90**, 1 (1993).
 - ²⁵ N. B. Kopnin, Phys. Rev. B **54**, 9475 (1996).
 - ²⁶ J. Koláček and P. Vašek, Physica C **336**, 199 (2000).
 - ²⁷ S. Ullah and A. T. Dorsey, Phys. Rev. B **44**, 262 (1991).
 - ²⁸ T. Nishio and H. Ebisawa, Physica C **290**, 43 (1997).
 - ²⁹ M. V. Feigelman, V. B. Geshkenbein, A. I. Larkin, and V. M. Vinokur, JETP Letters **62**, 834 (1995).
 - ³⁰ A. W. Smith, T. W. Clinton, W. Liu, C. C. Tsuei, A. Pique, Q. Li, and C. J. Lobb, Phys. Rev. B **56**, R2944 (1997).
 - ³¹ D. A. Beam, N. C. Yeh, and F. Holtzberg, J. Phys.: Condens. Matter **10**, 5955 (1998).
 - ³² R. Ikeda, Physica C **316**, 189 (1999).
 - ³³ N. B. Kopnin and A. V. Lopatin, Phys. Rev. B **51**, 15291 (1995).
 - ³⁴ T. Nagaoka, Y. Matsuda, H. Obara, A. Sawa, T. Terashima, I. Chong, M. Takano, and M. Suzuki, Phys. Rev. Lett. **80**, 3594 (1998).
 - ³⁵ H. Fukuyama, H. Ebisawa, and T. Tsuzuki, Prog. Theor. Phys. **46**, 1028 (1971).
 - ³⁶ R. Ikeda, T. Ohmi, and T. Tsuneto, J. Phys. Soc. Japan **60**, 1051 (1991).
 - ³⁷ L. G. Aslamazov and A. I. Larkin, Phys. Lett. **26A**, 238 (1968).
 - ³⁸ D. M. Ginsberg and J. T. Manson, Phys. Rev. B **51**, 515

- (1995).
- ³⁹ R. L. Neiman, J. Giapintzakis, D. M. Ginsberg, and J. M. Mochel, J. Supercond. **8**, 383 (1995).
 - ⁴⁰ W.E. Lawrence and S. Doniach, in *Proceedings of the 12th International Conference on Low Temperature Physics, Kyoto, 1970*, edited by E. Kanda (Keygaku, Tokyo, 1971), p. 361.
 - ⁴¹ A. Larkin and A. Varlamov, in *Physics of Conventional and Un-conventional Superconductors*, edited by K. Bennemann and J. B. Ketterson (Springer, Berlin, 2002).
 - ⁴² W. Lang, Physica C **226**, 267 (1994).
 - ⁴³ W. Lang, G. Heine, W. Kula, and R. Sobolewski, Phys. Rev. B **51**, 9180 (1995).
 - ⁴⁴ J. M. Harris, Y. F. Yan, and N. P. Ong, Phys. Rev. B **46**, 14293 (1992).
 - ⁴⁵ P. W. Anderson, Physica C **185-189**, 11 (1991).
 - ⁴⁶ K. Maki, Prog. Theor. Phys. **39**, 897 (1968).
 - ⁴⁷ A. A. Varlamov, G. Balestrino, E. Milani, and D. V. Livanov, Adv. Phys. **48**, 655 (1999).
 - ⁴⁸ W. Kula, W. Xiong, R. Sobolewski, and J. Talvacchio, IEEE Trans. Appl. Supercon. **5**, 1177 (1995).
 - ⁴⁹ S. Sarti, D. Neri, E. Silva, R. Fastampa, and M. Giura, Phys. Rev. B **56**, 2356 (1997).
 - ⁵⁰ N. B. Kopnin and V. M. Vinokur, Phys. Rev. Lett. **83**, 4864 (1999).
 - ⁵¹ G. G. N. Angilella, R. Pucci, A. A. Varlamov, and F. Onufrieva, Phys. Rev. B **67**, 134525 (2003).